P-Glycoprotein Kinetics Measured in Plasma Membrane Vesicles and Living Cells

Päivi Äänismaa and Anna Seelig*

Biophysical Chemistry, Biozentrum, University of Basel, Klingelbergstrasse 70, Switzerland

Received September 20, 2006; Revised Manuscript Received January 11, 2007

ABSTRACT: P-glycoprotein (MDR1, ABCB1) is an ATP-dependent efflux transporter of a large variety of compounds. To understand P-glycoprotein in more detail, it is important to elucidate its activity in the cellular ensemble as well as in plasma membrane vesicles (under conditions where other ATP dependent proteins are blocked). We measured P-glycoprotein activity in inside-out vesicles formed from plasma membranes of *MDR1*-transfected mouse embryo fibroblasts (NIH-MDR1-G185) for comparison with previous measurements of P-glycoprotein activity in living NIH-MDR1-G185 cells. In plasma membrane vesicles activity was measured by monitoring phosphate release upon ATP hydrolysis and in living cells by monitoring the extracellular acidification rate upon ATP synthesis via glycolysis. P-glycoprotein was stimulated as a function of the concentration with 19 structurally different drugs, including local anesthetics, cyclic peptides, and cytotoxic drugs. The concentrations of half-maximum P-glycoprotein activation, K_1, were identical in inside-out plasma membrane vesicles and in living cells and covered a broad range of concentrations ($K_1 \sim (10^{-8}-10^{-3})$ M). The influence of the pH, drug association, and vesicle aggregation on the concentration of half-maximum P-glycoprotein activation was investigated. The turnover numbers in plasma membrane vesicles and in living cells were also approximately identical if the latter were measured in the presence of pyruvate. However, in the absence of pyruvate they were higher in living cells. The rate of ATP hydrolysis/ATP synthesis decreased exponentially with decreasing free energy of drug binding from water to the transporter, $\Delta G^0_{tw(1)}$ (or increasing binding affinity). This suggests that drug release from the transmembrane domains has to occur before ATP is hydrolyzed for resetting the transporter.

P-glycoprotein, Pgp[1] (MDR1, ABCB1), is an ATP-dependent efflux transporter of a large variety of structurally diverse compounds, including toxins, drugs, and metabolites. Together with metabolizing enzymes and other efflux transporters with partially overlapping functions Pgp significantly contributes to a sophisticated cellular defense and housekeeping system (for review see refs *3*−*5*). Pgp consists of two homologous parts, each comprising a cytosolic, nucleotide-binding domain, NBD (*6*, *7*), and a drug-binding, transmembrane domain, TMD (*8*), which together form an integrated single entity as shown by preliminary X-ray data (*9*) and a recent homology model (*10*). Upon formation of the transition state each NBD carries one molecule of ATP which leads to a dimerization of the two domains. However, just one of the two ATP molecules seems to be hydrolyzed per dimerization event (*11*). The interplay between the NBDs and the TMDs upon drug stimulation is not yet fully understood. Whether ATP hydrolysis is required for driving the substrate across the membrane (*1*), or for resetting the transporter to the open starting position (after a passive transport step) (*12*), or even for both (*13*) is still a matter of intensive research.

The difficulty in understanding Pgp arises to a large extent from the fact that substrates are bound from the cytosolic membrane leaflet (*8*, *14*) (for review see refs *15*, *16*) and not from the aqueous phase as is the case in most well-known transporters. To reach the site of interaction the substrate has therefore first to partition from the aqueous phase (w) into the lipid phase (l). This process is described by the lipid−water partition coefficient, K_{lw}. Second, the substrate binds from the lipid phase to the activating (1) region of the TMDs (t), which is described by the transporter−lipid binding constant, $K_{tl(1)}$. As a consequence, the binding constant describing substrate binding from the aqueous phase to the activating binding region of the transporter, $K_{tw(1)}$, can be expressed as the product of the lipid−water partition coefficient, K_{lw}, and the transporter−lipid binding constant, $K_{tl(1)}$ ($K_{tw(1)} = K_{lw} \cdot K_{tl(1)}$). Analogous binding constants can be defined for the inhibitory (2) binding region of the transporter. Substrate binding thus strongly depends on the lipid−water partition coefficient, K_{lw}, of the compound which in turn depends on the lateral packing density of the lipid membrane, π_M, and the pH of the environment (for detail see refs *5*, *17*).

In inside-out membrane vesicles drugs merely have to intercalate between the lipids with the polar head group remaining in the head group region of the membrane, whereas in living cells they have to diffuse across the

* Corresponding author. Phone: +41-61-267 22 06. Fax: +41-61-267 21 89. E-mail: Anna.Seelig@unibas.ch.

[1] Abbreviations: CMC_D, critical micelle concentration of drug; ECAR, extracellular acidification rate; K_1 (K_2), aqueous substrate concentration at half-maximum Pgp activation (inhibition); K_{lw}, lipid−water partition coefficient; $K_{tl(1)}$ ($K_{tl(2)}$), binding constant of the drug from the lipid membrane to the activating (inhibitory) binding region of the transporter; $K_{tw(1)}$ ($K_{tw(2)}$), binding constant of the drug from water to the activating (inhibitory) binding region of the transporter; MDR, multidrug resistance; NBD, nucleotide binding domain; Pgp, P-glycoprotein-ATPase (MDR1, ABCB1); TMD, transmembrane domain; V_1 (V_2), maximum (minimum) Pgp activity.

10.1021/bi0619526 CCC: $37.00
Published on Web 02/16/2007

membrane. Permanently charged cationic compounds such as spin labeled verapamil (*18*) can, therefore, reach the Pgp binding site in inside-out vesicles but not in living cells.

Pgp activity has generally been measured in plasma membrane vesicles of *MDR1*-transfected cells or in reconstituted proteoliposomes which both expose the NBDs to the extravesicular side and allow monitoring the release of inorganic phosphate (*1*, *19*, *20*) or ADP (*20*, *21*) upon drug stimulation. In living cells Pgp stimulation with drugs leads to intracellular ATP hydrolysis which entails enhanced ATP synthesis via glycolysis, whereby lactic acid is produced as waste product and is excreted by the cell (*22*). We exploited this process to monitor Pgp activity as a function of drug concentration in real time (*2*, *23*, *24*) using a Cytosensor microphysiometer (*25*). The experiments have shown that Pgp activity in living cells is not only controlled by the nature and the concentration of the drug, and the packing density of the membrane, but also by the metabolic state of the cell (*2*).

A comparison of Pgp activity in living cells and in inside-out membrane vesicles of the same cells has so far been published only for verapamil (*2*). Since the two systems bear distinct differences we extended the comparison to the 15 drugs measured previously in living mouse embryo fibroblasts (NIH-MDR1-G185) (*24*) and added four additional drugs to get an even broader selection of compounds. The 19 compounds range from local anesthetics (MW $\approx$ 200 g/mol) to cyclic peptides (MW $\approx$ 1200 g/mol) and include cytotoxic drugs. The wide variety of compounds allows, then, testing how the binding affinity of the drug for the TMDs influences the rate of nucleotide hydrolysis at the NBDs.

We show that the concentrations of half-maximum Pgp activation, K_1, in living *MDR1*-transfected mouse embryo fibroblasts (*24*) are identical to those in inside-out plasma membrane vesicles of the same cells, provided the two systems are at the same pH and possible artifacts due to drug and vesicle association are taken into account. The relative rates of activation are linearly correlated. The turnover numbers are practically identical if Pgp activity in living cells is measured in the presence of pyruvate (*2*, *24*). In the absence of pyruvate Pgp activity in living cells is higher. The maximum rate of Pgp activity, $\ln(V_1)$, decreased linearly with increasing affinity of the drug from water to the TMDs. Drug release is thus the rate-determining step and the transporter can only be reset if it is unloaded at the extracellular side.

MATERIALS AND METHODS

Materials. Amitriptyline·HCl, *cis*-flupenthixol·2HCl, daunorubicin·HCl, dibucaine·HCl, diltiazem·HCl, lidocaine·HCl, progesterone, promazine·HCl, trifluoperazine·2HCl, triflupromazine·HCl, and vinblastine·H_2SO_4 were from Sigma-Aldrich (Steinheim, Germany), and (*R*/*S*)-verapamil·HCl and colchicine were from Fluka (Buchs, Switzerland). Chlorpromazine·HCl and reserpine·HCl·H_2O were generous gifts from Merck (Darmstadt, Germany), and cyclosporin A, PSC-833, and glivec mesylate were generous gifts from Novartis AG (Basel, Switzerland). The inhibitor OC144-093 was a gift from Dr. T. Litman. Complete EDTA-free protease inhibitor cocktail tablets were obtained from Roche Diagnostics (Mannheim, Germany), 1,4-dithiol-DL-threitol, DTT, from Applichem (Darmstadt, Germany), and bicinchoninic acid, BCA, protein assay reagents from Pierce (Rockford, IL). All other chemicals were from either Sigma, Fluka, or Merck. Cell culture media DMEM with and without pyruvate (liquid and dry, Cat. No. 21969 and Cat. No. 52100, respectively) as well as other compounds required for cell culture such as fetal bovine serum, FBS, L-glutamine, and antibiotics were from Gibco-BRL (Basel, Switzerland).

Cell Lines and Cell Culture. Wild-type (NIH3T3) and *MDR1*-transfected mouse embryo fibroblasts (NIH-MDR1-G185) were generous gifts from Dr. M. M. Gottesman and Dr. S. V. Ambudkar (The National Institutes of Health, Bethesda, MD). Cells were grown in the presence of 0.15 μM colchicine and were maintained as described previously (*2*, *23*).

Plasma Membrane Preparation. The crude plasma membrane vesicles were prepared as described previously with some modifications (*2*, *26*). Briefly, cells grown in 15 cm dishes were washed once with PBS buffer, and then scraped into ice-cold PBS (pH 7.0 at ambient temperature) supplemented with protease inhibitors (1 tablet/50 mL PBS). Next, cells were washed with ice-cold buffer A by centrifugation at 1000g_{max} for 10 min at 4 °C. Buffer A consisted of 10 mM Tris-HCl, 10 mM NaCl, 1 mM $MgCl_2$, protease inhibitors (1 tablet/50 mL), adjusted to pH 7.5 at ambient temperature. The pellet was resuspended in buffer A (5 mL/4*15 cm dishes) and was then kept on ice until disruption with a "One Shot" cell disrupter (Constant Systems Ltd, Warwickshire, U.K.) at 400 bar. The "One Shot" cell disrupter uses pressure to force a sample through a small fixed orifice at high speed. By transferring the cell sample from a region of high pressure to one of low pressure cells disrupt. The cell lysate was diluted 1:1 with ice-cold buffer B (10 mM Tris-HCl, 50 mM *N*-methyl-D-glucamine, NMDG, 120 mM sucrose, protease inhibitors (1 tablet/50 mL), adjusted to pH 7.4 at ambient temperature). The unbroken cells and nuclei were then precipitated by centrifugation at 800g_{max} for 10 min at 4 °C. Subsequently mitochondria were removed by centrifugation at 6000g_{max} for 10 min at 4 °C, and in the final centrifugation step (100000g_{max}, 1 h, 4 °C) the crude membranes were pelleted. The pellet was resuspended in buffer B and homogenized by repeated aspiration through a 23-gauge syringe. Aliquots were rapidly frozen in dry ice and stored at −80 °C until use.

The average protein content of the plasma membrane vesicles from five different preparations was determined as ((9.9 $\pm$ 1.7) mg/mL) using the BCA protein assay with bovine serum albumin (fraction V) as a standard. The initial number of cells per preparation varied from 5.7×10^8 to 1.1×10^9. Western immunoblots made with supernatants and pellets of the different centrifugation steps after cell disruption (800g_{max}, 6000g_{max}, 100000g_{max}) suggest a substantial loss of Pgp. Pgp was detected with monoclonal antibody C219. The total loss of plasma membrane Pgp during membrane vesicle preparation was estimated as approximately 20%. Taking into account the number of Pgp molecules in NIH-MDR1-G185 cells determined previously as $(1.95 \pm 0.53) \times 10^6$ Pgp/cell (*27*), the molecular weight (170 kDa), and a total loss of Pgp ($\sim$20%), the amount of Pgp per total protein concentration was estimated as (1.1 $\pm$ 0.3)% (average of five different membrane preparations).

Table 1: The Critical Micelle Concentration of Drugs, CMC_D, the Stock Solution Concentrations, and the Highest Drug Concentrations Measured in Phosphate Release (P_i) Assay and in ECAR Measurements

no.	compound	CMC_D[a] [mM]	stock solution ECAR [mM]	highest measd ECAR[d] [mM]	stock solution P_i assay [mM]	highest measd P_i assay [mM]
1	amitriptyline	5.0	0.4[b]	0.064	10.6[e]	0.887
2	chlorpromazine	0.96	0.2[b]	0.011	2.6[e]	0.216
3	*cis*-flupenthixol	0.16	0.06[b]	0.012	1.5[e]	0.126
4	cyclosporin A	~0.001	0.002[c]	0.002	0.07,[f] 0.42[f]	0.001,[h] 0.007[h]
5	daunorubicin	0.06 − 0.3[j]	0.1[b]	0.087	0.096,[e] 0.48,[f] 0.9[e]	0.008, 0.008,[h] 0.075
6	dibucaine	2.4	0.2,[b] 1.0[b]	0.059	0.47,[e] 2.3[e]	0.039, 0.191
7	diltiazem	10	0.6[b]	0.498	10.2[e]	0.833
8	glivec	~1	0.1[b]	0.092	1.8[e]	0.151
9	lidocaine	60	1.0[b]	0.939	24,[e] 90[e]	2.0, 7.5
10	progesterone	0.08	0.2[c]	0.029	10[f]	0.167[h]
11	promazine	7	0.4[b]	0.227	3.45[e], 27.8[e]	0.287, 2.3
12	(*R*/*S*)-verapamil	5	0.1[c]	0.058	0.66,[e] 1.9[e]	0.055, 0.160
13	reserpine	0.009	0.01,[c] 0.008[c]	0.003	0.55[f]	0.009[h]
14	trifluoperazine	0.18	0.1[b]	0.009	0.4,[e] 2.0[e]	0.033, 0.166
15	triflupromazine	0.47	0.1[b]	0.011	1.7,[e] 2.0[e]	0.143, 0.166
16	colchicine	2.6	nd	nd	200[f]	3.3[h]
17	OC144-093	~0.002	nd	nd	0.06[f]	0.001[h]
18	PSC-833	~0.001	nd	nd	0.2,[f] 0.8[f]	0.001[h]
19	vinblastine	0.1	0.1[c]	0.076	0.33[g]	0.027[i]

[a] CMC_D determined by surface activity measurements in 50 mM Tris-HCl, 114 mM NaCl, pH 7.4 at ambient temperature. [b] Stock solution in DMEM flow medium. [c] Stock solution in DMEM flow medium containing 0.5% (v/v) DMSO. [d] Drug concentrations after correction for adsorption. [e] Stock solution in water. [f] Stock solution in 100% (v/v) DMSO. [g] Stock solution in 6% (v/v) DMSO. [h] Drug concentration containing 1.7% (v/v) DMSO. [i] Drug concentration containing 0.5% (v/v) DMSO. [j]Depending on stock solution concentration.

The orientation of Pgp in plasma membrane vesicles was tested by permeabilizing the membranes with CHAPS in order to unmask the occluded nucleotide binding domains (*28*). Since increasing concentrations of CHAPS did not lead to an increase in the rate of ATP hydrolysis, we concluded that the vesicles obtained by the "One-Shot" procedure exhibited an essentially inside-out orientation.

Phosphate Release Assay. The Pgp associated ATPase activity was determined according to Litman et al. (*19*) in a 96-well microtiter plate (Nunc F96 MicroWell plate, non-treated) with small modifications. The plasma membrane vesicles were diluted to a protein concentration of 0.1 mg/mL in ice-cold phosphate release assay buffer which consisted of 25 mM Tris-HCl including 50 mM KCl, 3 mM ATP, 2.5 mM $MgSO_4$, 3 mM DTT, 0.5 mM EGTA, 2 mM ouabain, and 3 mM sodium azide, adjusted to pH 7.0 at 37 °C, unless stated otherwise. Each series of experiments contained 5 μg of protein per total assay volume of 60 μL (total protein concentration 84.7 μg/mL per sample). Incubation with the various drugs was started by transferring the plate from ice to a water bath at 37 °C for 1 h, and was terminated by rapidly cooling the plate on ice. The inorganic phosphate, P_i, released was determined by addition of ice-cold solution (200 μL) containing ammonium molybdate (0.2% (w/v)), sulfuric acid (1.43% (v/v)), freshly prepared ascorbic acid (1% (w/v)), and SDS (0.9% (w/v)) to each well. After incubation at room temperature (30 min), the phosphate released was quantified colorimetrically at 820 nm using a micro-plate reader Spectramax M2 (Molecular Device, Sunnyvale). Reference standards were included to each 96-well plate. Samples incubated with 0.5 mM vanadate to determine the vanadate-sensitive Pgp activation were obtained in parallel and were subtracted from the measured values.

Cytosensor Measurements. The rate of ATP synthesis in living cells was measured by monitoring the extracellular acidification rate, ECAR, using a Cytosensor (*25*). The ECAR was shown to correspond to the rate of lactate efflux as a result of glycolysis (for details cf. refs *2*, *23*, *24*). The DMEM flow medium used was buffered with phosphate (0.91 mM) and thus exhibited a very low buffer capacity. Moreover, it contained pyruvate (1 mM) which reduces the basal activity of cells by (50−60)% (*2*). Measurements were performed at pH 7.4 and $T = 37$ °C. The transformation of the voltage per time data ($\mu V \cdot s^{-1}$) to protons released per cell per second ($H^+ \cdot cell^{-1} \cdot s^{-1}$) was performed as described previously (*2*).

Stock Solutions of Drugs. Stock solutions for the phosphate release assay were made with nanopure water or DMSO (cf. Table 1). Drug solutions were prepared by further dilution of the stock solution with either water or DMSO. The measured drug concentrations were then obtained by adding 5 μL of aqueous drug solution or 1 μL of DMSO drug solution into the phosphate release assay buffer (total sample volume per well = 60 μL). The final DMSO concentration was constant $c = 1.7\%$ (v/v).

Stock solutions for Cytosensor measurements were made with DMEM flow medium or DMSO which was diluted with flow medium to the final DMSO concentration (0.5% (v/v)). Upon further dilution the DMSO concentration was decreasing. Stock solution concentrations and the highest concentrations measured with the two assays are included in Table 1. At the concentrations applied DMSO affected neither the ECAR (*24*) nor the phosphate release rate.

All drugs investigated are amphiphilic and form micelle-like associates at high concentrations. The critical micelle concentrations of drugs, CMC_D, determined previously by surface activity measurements in 50 mM Tris-HCl buffer containing 114 mM NaCl (pH 7.4 at ambient temperature) are given in Table 1 (refs *29*, *30* and X. Li-Blatter and A. Seelig, unpublished results). For comparison the CMC_D value of trifluprazine was also measured in the phosphate release assay buffer (pH 7.4 at ambient temperature) and was found to be very similar. The stock solution concentra-

tions were below the critical micelle concentration, CMC_D, for most drugs in ECAR measurements but not in the phosphate release assay (see Table 1). The direct injection of the concentrated solutions into small volumes (60 μL) of ice-cold buffer containing the membrane vesicles generated high local drug concentrations. Since the pH of the buffer increases with decreasing temperature (pH 7.9 at $T = 4$ °C), this may have led to irreversible drug association in some cases which reduces membrane partitioning, and, in turn, binding to Pgp. Drugs which are especially prone to association are colchicine, progesterone, daunorubicin, and phenothiazines.

Drug Adsorption. Some drugs strongly adsorb to plastic surfaces (*31*). Drug solutions reaching the measuring cell in the Cytosensor were therefore corrected for adsorption using UV spectroscopy (for details see ref *24*). Adsorption varied strongly from compound to compound and was relatively small for verapamil (~21% for verapamil (20 μM)) and high for phenothiazines (~89.5% for triflupromazine (50 μM)). The corresponding values for adsorption to the test tubes (polypropylene) used in the phosphate release assay were also determined (as ~3% (per 120 min) for verapamil (40 μM) and as ~19.0% (per 130 min) for triflupromazine (23 μM)) but were not taken into account.

90° Light Scattering. Light scattering at 90° was measured with a Hitachi F-4500 spectrofluorometer under constant stirring at an excitation and emission wavelength of 550 nm ($T = 37$ °C). A quartz cuvette with a cell length of 1 cm and a volume of 3.5 mL was used. It was filled with 1.8 mL of phosphate release assay buffer (pH 7.0 at 37 °C) containing crude plasma membrane vesicles with the same protein concentration as used in the phosphate release assay (84.7 μg/mL). Aliquots (μL) of a promazine stock solution prepared in nanopure water (6.24, 12.4, 25.7, and 27.3 mM) were added into the buffer. The results were corrected for dilution (maximally ~10%) upon promazine titration by titrating equal amounts of nanopure water into the membrane-containing phosphate release assay buffer.

The Kinetic Model. We used a modified Michaelis−Menten model (eq 1) proposed by Litman et al. (*19*) for data evaluation. It assumes basal Pgp activity in the absence of drugs, activation upon drug binding to a first binding region at low drug concentrations, and inhibition upon drug binding to a second binding region at high drug concentrations. The rate of Pgp activity, V_{sw}, is expressed as follows:

$$V_{sw} = \frac{K_1K_2V_0 + K_2V_1C_{sw} + V_2C_{sw}^2}{K_1K_2 + K_2C_{sw} + C_{sw}^2} \qquad (1)$$

where C_{sw} is the substrate concentration in aqueous solution, V_0 is the basal activity in the absence of drugs, K_1 and K_2 are the concentrations of half-maximum activation and inhibition, respectively, V_1 is the maximum rate of ATP hydrolysis, and V_2 is the minimum rate of ATP hydrolysis at infinite substrate concentration. The corresponding reaction scheme was shown previously (*24*). At low substrate concentrations eq 1 reverts to the simple Michaelis−Menten kinetics which is illustrated in reaction 1, Scheme 1, where S_w is the substrate in the aqueous phase, S_l is the substrate in the lipid phase, k_0 and k_{-0} are the partitioning rate constants, and $K_{lw} = k_0/k_{-0}$ is the lipid−water partition coefficient. ATP and the substrate, S_l, bind to the transporter, T, to form the $T(ATP)S_t$ complex. S_t is the substrate bound to the activating binding region of the transporter, k_1 and k_{-1} are the rate constants for association to and dissociation from the activating binding region, and $K_{tl(1)} = k_1/k_{-1}$ is the binding constant of the substrate for the activating binding region of the transporter within the lipid membrane, under the assumption that the association/dissociation reactions are rapid compared to catalytic step; k'_{cat} is the catalytic rate constant, and S_{rel} is the substrate released. For simplicity only one ATP (ADP) molecule per Pgp is shown. As seen in reaction 2 under the anaerobic conditions in the Cytosensor one molecule of glucose is transformed to two molecules of ATP and two molecules of lactic acid which is then exported out of the cell. The synthesis of ATP comprises several steps, and k'_{lac} is the over-all catalytic rate constant.

Scheme 1

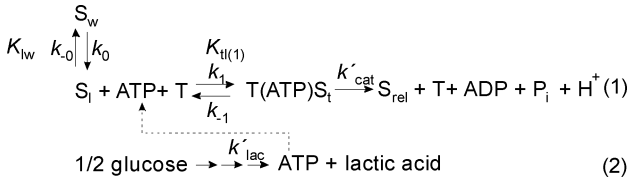

RESULTS

Basal Pgp Activity. For calibration, the time dependence of phosphate release upon Pgp activation at 37 °C was measured in plasma membrane vesicles of *MDR1*-transfected mouse embryo fibroblasts (NIH-MDR1-G185) in the presence and absence of 0.5 mM vanadate and 31.7 μM verapamil, respectively (Figure 1A,B). Samples were analyzed every 15 min, and the reaction was stopped by cooling the samples on ice. The amount of phosphate released was determined as described in Materials and Methods. ATP hydrolysis as a function of time was linear under each condition throughout the time period investigated (75 min). The phosphate release assay buffer contains sodium azide, ouabain, and EGTA to inhibit, e.g., Na/K- and Ca-ATPases, which reduced the basal activity of all ATP consuming enzymes by 75.1% in comparison to a buffer lacking these inhibitors. Sodium azide had the strongest effect (results not shown).

The ATPase activity of plasma membrane vesicles in phosphate release assay buffer is shown in Figure 1A (open triangles). Addition of verapamil (31.7 μM) increased the hydrolysis of ATP by Pgp (solid squares). In the presence of vanadate (0.5 mM) the release of phosphate was reduced (open down triangles) and remained at the same level upon addition of verapamil (open squares), indicating that Pgp activity was inhibited by vanadate (Figure 1A). The remaining phosphate released arises most likely from the ATPase activity of enzymes that are not sensitive to the inhibitors used. Figure 1B shows the vanadate-sensitive basal and verapamil-stimulated ATPase activity (assumed to correspond to the ATPase activity of Pgp) as a function of the incubation time at 37 °C. In the following, a single time point measurement (60 min) of Pgp activity was used. For five different plasma membrane preparations the average vanadate-sensitive basal Pgp activity expressed as phosphate released per total protein concentration and time was

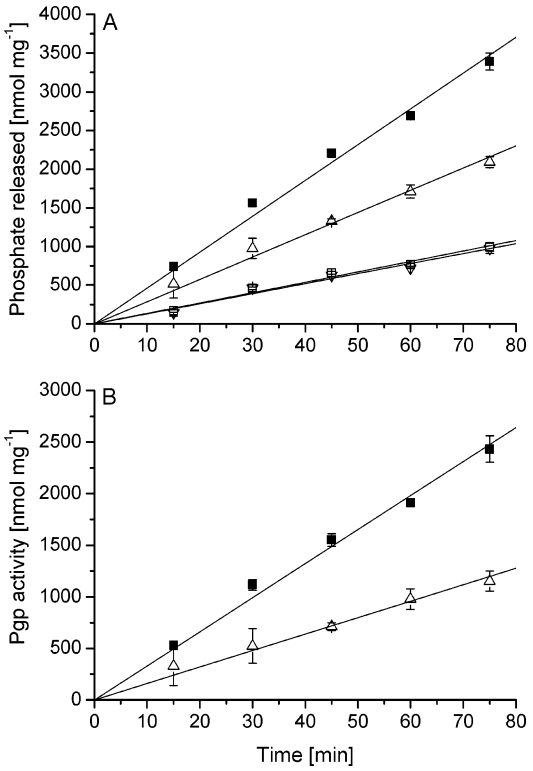

FIGURE 1: Time dependence of vanadate-sensitive Pgp activity in plasma membranes from NIH-MDR1-G185 cells in the presence of verapamil (31.7 μM) and vanadate (0.5 mM). A: Phosphate release measurements were made under four different conditions: in the absence of verapamil and vanadate (△), in the presence of verapamil and in the absence of vanadate (■), in the absence of verapamil and in the presence of vanadate (▽), and in the presence of verapamil and vanadate (□). B: Vanadate-sensitive Pgp activity in the presence (■) and in the absence of verapamil (△). Values are expressed as the mean of three measurements ± SD. The solid lines are the linear regressions to the data. For further analysis a single time point measurement (60 min) of Pgp activity was used.

determined as $V_0 = (12.3 \pm 1.3)$ nmol·mg^{-1}·min^{-1} ($n \approx 126$).

Drug-Stimulated Pgp Activity Profiles Measured in Plasma Membrane Vesicles of MDR1-Transfected Mouse Embryo Fibroblasts. Pgp activity in inside-out plasma membranes vesicles of NIH-MDR1-G185 cells was measured for the 19 drugs listed in Tables 1 and 2. Figure 2A−D shows the rate of Pgp activity as a function of the substrate concentration in aqueous solution (Log scale). Drug-stimulated Pgp activity is expressed as percentage of the basal activity (taken as 100%).

Maximum Pgp activity requires high millimolar concentrations for very hydrophilic drugs, e.g., lidocaine (Figure 2A, filled squares) and colchicine (Figure 2C, filled down triangles), micromolar concentrations for more hydrophobic drugs, e.g., *cis*-flupentixol (Figure 2A, filled triangles) and verapamil (Figure 2B, filled squares), and nanomolar concentrations for even more hydrophobic drugs, e.g., OC144-093 (Figure 2D, open circles). Compounds of intermediate hydrophobicity show the characteristic bell-shaped Pgp activity profiles as a function of concentration observed previously in living NIH-MDR1-G185 cells (*24*). For very hydrophilic compounds inhibition could not be reached, whereas for the very hydrophobic compounds activation is barely visible or not present at all. The solid lines in Figure 2A−D are fits to the modified Michaelis−Menten model (eq 1) proposed by Litman et al. (*19*) (for details see ref *24*). The kinetic parameters derived from phosphate release measurements in plasma membrane vesicles are summarized in Table 2.

Vesicle Aggregation Can Hamper Measurement of the Inhibitory Part of the Pgp Activity Profile. The inhibitory part of the activity profile was easily reached in the ECAR assay (*24*). In the phosphate release assay this was more difficult since the highly concentrated drug solutions used in the phosphate release assay can lead to drug association as outlined in Materials and Methods; moreover, vesicle aggregation can occur as will be shown below.

In the absence of drugs inside-out membrane vesicles exhibit a negative surface potential, ψ, which prevents their aggregation. Upon partitioning of positively charged drugs, the negative surface potential decreases or even disappears (*24*, *32*), which can lead to vesicle aggregation. To investigate this phenomenon in more detail three compounds (verapamil, chlorpromazine, and promazine) with high lipid−water partition coefficients, K_{lw} (*24*), and high pK_a values were chosen and 90° light scattering measurements were performed in parallel to the spectroscopic phosphate release assay. Figure 3A−C displays the raw data of the phosphate release assay made with plasma membrane vesicles of *MDR1*-transfected and wild-type cells in the presence and absence of vanadate (0.5 mM) and drug. Plasma membrane vesicles of wild-type cells show some residual vanadate-sensitive activity in the presence of sodium azide, ouabain, and EGTA (Figure 3A−C) which is most likely due to a low concentration of Pgp (*2*). Nonenzymatic ATP hydrolysis was not observed.

At high drug concentrations the plasma membrane vesicles of wild-type and *MDR1*-transfected cells with and without vanadate both show a decrease in the optical density (820 nm). The effect increases in the order verapamil (pK_a 8.9) ≤ chlorpromazine (pK_a 9.2) < promazine (pK_a 9.4). As seen in Figure 3C a concomitant increase in light scattering intensity was observed at promazine concentrations, $C > 10^{-4}$ M. At even higher concentrations, $C > 7 \times 10^{-4}$ M, light scattering started to increase strongly not only with concentration but also with time, suggesting the formation of larger aggregates. As seen in Figure 3A−C the aggregation phenomenon was independent of the presence of Pgp and was merely a result of charge neutralization of inside-out cellular vesicles of wild-type and *MDR1*-transfected cells which exhibit approximately the same negative surface potential (cf. footnote 1 in ref *24*). Vesicle aggregation most likely hampered drug access to the membrane and ATP binding to the NBDs. Partitioning of electrically neutral drugs (progesterone, cyclosporin A, and PSC-833) or cationic drugs with low pK_a values (reserpine, glivec, daunorubicin, and OC144-093) (Figure 2A−D) induced no vesicle aggregation even at high concentrations (data not shown). Since problems due to drug association, as well as vesicle aggregation, are less pronounced at pH 7.0 than at pH 7.4, we chose the lower pH for the phosphate release assay despite the fact that the ECAR measurements were performed at pH 7.4.

The Influence of pH on the Kinetic Parameters of Drug-Stimulated Pgp Activity. To investigate the influence of the pH on Pgp activity we chose three representative examples, the electrically neutral progesterone and the cationic com-

Table 2: Kinetic Parameters of Pgp Activation for 19 Drugs. The Concentration of Half-Maximum Activation (Inhibition), K_1 (K_2), and the Maximum (Minimum) Transporter Activity, V_1 (V_2), Obtained from Phosphate Release Measurements in Plasma Membrane Vesicles of NIH-MDR1-G185 Cells[a]

no.	compound	MW_{base} [g/mol]	pK_a[c]	K_1 [μM]	K_2 [μM]	V_1 [fold]	V_2 [fold]	no. of experiments
1	amitriptyline	277.4	9.4	14.2 ± 0.7	1239.5 ± 110.5	2.3 ± 0.1	1.1 ± 0.2	3
2	chlorpromazine	318.9	9.2	10.5 ± 0.5	125.0 ± 15.0	2.2 ± 0.1	1.2 ± 0.1	2
3	*cis*-flupenthixol	434.5	7.8	1.8 ± 0.6	28.3 ± 5.8	2.4 ± 0.1	0.3 ± 0.1	3
4	cyclosporin A	1202.6		0.02 ± 0.01	1.5 ± 1.0	0.9 ± 0.1	0.4 ± 0.2	3
5	daunorubicin	527.5	8.4	5.5 ± 1.5	43.5 ± 3.5	1.4 ± 0.1	0.8 ± 0.1	2
6	dibucaine[b]	343.5	8.5	4.1 ± 0.9	nd	2.9 ± 0.2	nd	4
7	diltiazem	414.5	8.9	6.7 ± 1.3	1678.5 ± 1.5	3.2 ± 0.1	1.0 ± 0.1	2
8	glivec	493.6	8.07	1.2 ± 0.3	241.8 ± 49.4	1.6 ± 0.1	0.10 ± 0.02	2
9	lidocaine	234.3	7.6	1630 ± 70	nd	2.7 ± 0.1	nd	4
10	progesterone	314.4		13.9 ± 0.4	144.7 ± 27.3	3.3 ± 0.2	0.7 ± 0.4	4
11	promazine	284.4	9.42	82.0 ± 10.0	2150 ± 200	2.5 ± 0.1	0.1 ± 0.0	2
12	(*R*/*S*)-verapamil	454.6	8.92	1.0 ± 0.3	843.6 ± 159.1	2.5 ± 0.1	1.0 ± 0.4	15
13	reserpine	608.7	6.6	0.2 ± 0.1	1.0 ± 0.2	1.7 ± 0.2	1.0 ± 0.1	2
14	trifluoperazine	407.5	8.09	2.3 ± 0.2	58.3 ± 14.4	2.4 ± 0.2	1.0 ± 0.2	5
15	triflupromazine	352.4	9.1	8.0 ± 2.7	140.0 ± 26.5	2.0 ± 0.1	1.0 ± 0.2	4
16	colchicine	399.4		227.6 ± 20.1	nd	1.7 ± 0.1	nd	2
17	OC144-093	494.7	6.3	0.008 ± 0.002	0.95 ± 0.15	0.9 ± 0.1	0.3 ± 0.1	2
18	PSC-833	1214.6		0.008 ± 0.001	2.6 ± 0.1	0.8 ± 0.1	0.4 ± 0.1	4
19	vinblastine	811.0	7.4	1.6 ± 0.2	40.5 ± 4.5	1.8 ± 0.1	0.9 ± 0.1	2

[a] Kinetic parameters for the inhibitory part of the Pgp activation profiles, K_2 and V_2, have to be taken as the estimates because for many compounds the inhibitory part is affected by vesicle aggregation and drug association appearing at high drug concentrations (discussed in detail in text). [b] Data fitted to simple Michaelis−Menten equation. [c] For references of pK_a values see ref *24*; the pK_a values for OC144-093 and vinblastine are taken from SciFinder and Merck Index, respectively.

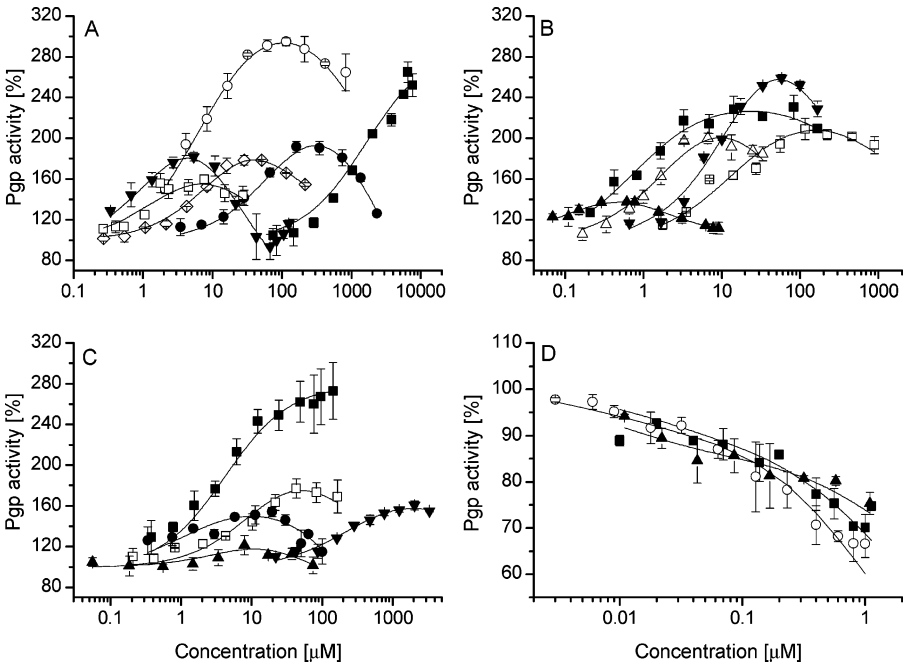

FIGURE 2: Vanadate-sensitive Pgp activity profiles obtained from phosphate release measurements in plasma membrane vesicles of NIH-MDR1-G185 cells. Measurements were performed at $T = 37$ °C and at pH 7.0. A: Chlorpromazine (◇), *cis*-flupenthixol (▼), diltiazem (○), lidocaine (■), promazine (●), and vinblastine (□). B: Amitriptyline (□), progesterone (▼), reserpine (▲), trifluoperazine (△), and verapamil (■). C: Daunorubicin (▲), dibucaine (■), colchicine (▼), glivec (●), and triflupromazine (□). D: Cyclosporin A (■), PSC-833 (▲), and OC144-093 (○). Data are expressed as the average of at least two measurements. Solid lines are fits to the modified Michaelis−Menten equation (eq 1), except for dibucaine, which is fitted to the simple Michaelis−Menten equation ($V_{sw} = V_0 + (V_{max} - V_0)C_{sw}/(K_M + C_{sw})$, where V_{max} is the maximum activity and K_M the Michaelis−Menten constant).

pounds, promazine (pK_a 9.4) and verapamil (pK_a 8.9). The pH dependence of Pgp activity as a function of concentration was investigated in the range of pH 6.2 to pH 7.4 at 37 °C using the phosphate release assay (Figure 4A,B). The basal Pgp activity, V_0, does barely change in the pH range investigated (Figure 4A), which is in good agreement with previous experiments (*33*).

For the uncharged progesterone the maximum activity, V_1 (Figure 4A), and the concentration of half-maximum activation, K_1 (Figure 4B), were practically identical at two different pH values. However, for verapamil and promazine the maximum activity, V_1, increased with increasing pH (Figure 4A) and the concentration of half-maximum activation, K_1, decreased (Figure 4B). This is due to an increase

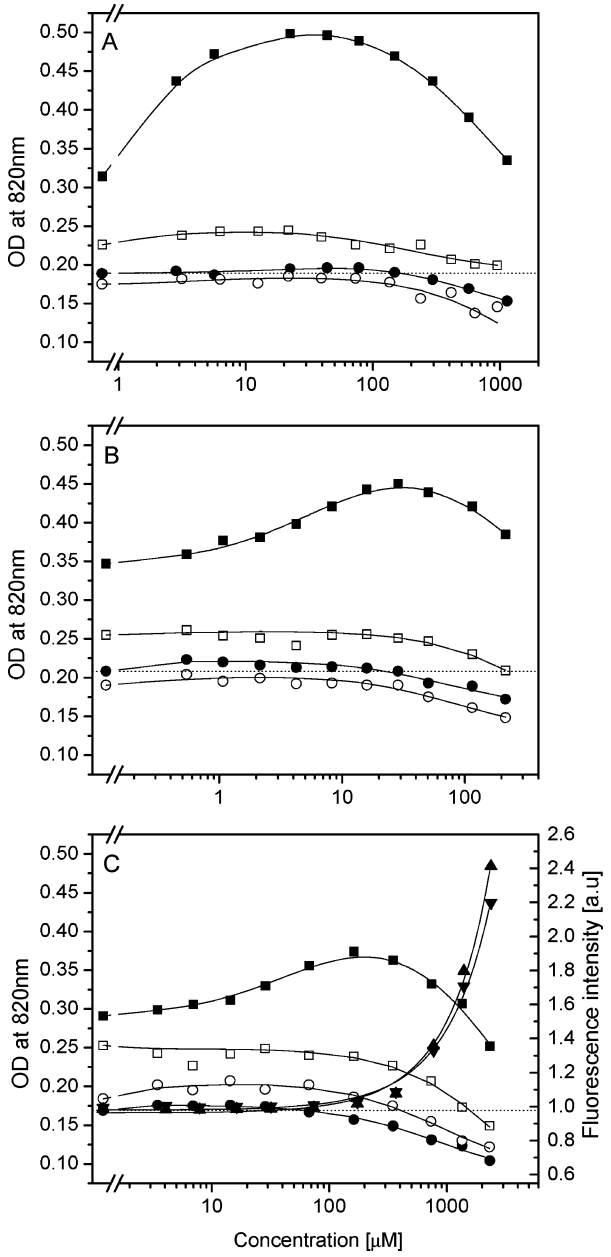

FIGURE 3: The amount of ATP hydrolyzed in plasma membrane vesicles of wild-type (open symbols, □, ○)) and NIH-MDR1-G185 cells (filled symbols, ■, ●) with increasing concentration of verapamil (A), chlorpromazine (B), and promazine (C). Circles (○, ●) refer to measurements in the presence of 0.5 mM vanadate and squares (□, ■) in the absence of 0.5 mM vanadate. The results are expressed as optical densities at 820 nm (A−C, labels on left-hand side). The solid lines are fits to the modified Michaelis−Menten equation (eq 1). Labels at right-hand side in (C): 90° light scattering intensity at 550 nm as function of increasing concentration of promazine in the membrane-containing phosphate release assay buffer in the absence of 0.5 mM vanadate (▼) and in the presence of 0.5 mM vanadate (▲). Light scattering intensities are normalized to the light scattering intensity of the sample without promazine. Data were fitted to an exponential curve. All measurements were performed at $T = 37$ °C and pH 7.0.

in the fraction of unprotonated drug and, in turn, to an increase in membrane partitioning and Pgp binding.

ECAR Measurements with Cytotoxic Compounds. The basal ECAR of NIH-MDR1-G185 cells in pyruvate containing DMEM flow medium was determined as $V_0 = ((1.4 \pm 0.6) \times 10^7)$ $H^+ \cdot cell^{-1} \cdot s^{-1}$ ($n = 74$ measurements, passage number >4). In the absence of pyruvate the value is at least

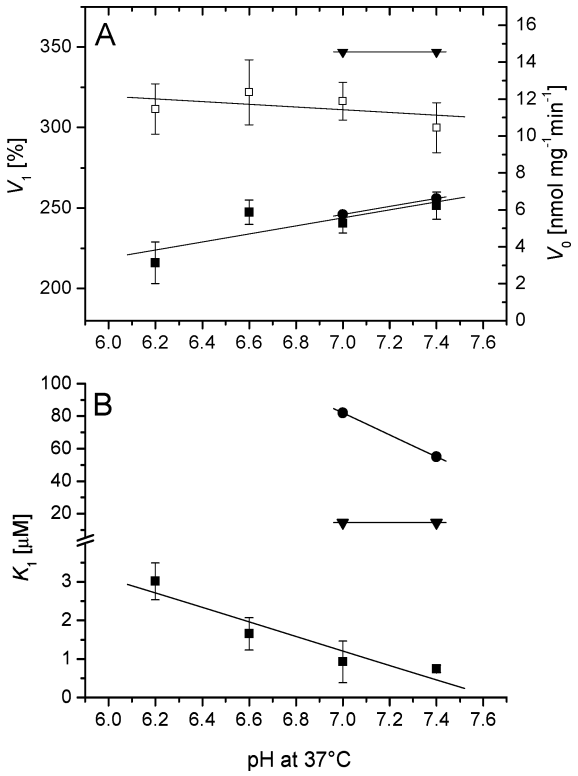

FIGURE 4: The effect of pH. A: Basal Pgp activity, V_0 (□) (labels at the right-hand side), and maximum Pgp activity, V_1 (labels at left-hand side), for verapamil (■), promazine (●), and progesterone (▼) as a function of pH. B: Concentration of half-maximum Pgp activation, K_1, as a function of pH. Phosphate release measurements were performed in either 25 mM Tris-HCl or 25 mM Hepes-KOH buffer at 37 °C. The pH of phosphate release assay buffer was adjusted taking into account the temperature coefficient of the buffer. Data are expressed as the average of two to four measurements. Solid lines are linear regressions to the data. For data evaluation the average basal activity value in the pH range (pH 6.2 to pH 7.4) was used.

twice as large as shown previously (*2*). Figure 5A shows the stimulation of *MDR1*-transfected and wild-type cells with a single concentration of vinblastine (22.9 μM). First, cells were perfused with drug-free DMEM flow medium until a stable ECAR was reached. The first two points in Figure 5A correspond to the ECAR at the end of the equilibration phase (∼1 h) and were taken as basal values (100%). The ECAR comprises all the metabolic effects of the cell including basal Pgp activity. Cells were then stimulated for 3 min with vinblastine (hatched bar) during which two ECAR measurements (first and second stimulation point) were performed. The second stimulation point indicated as a solid symbol was used for the evaluation of Pgp activity (*24*). Cells were then again flushed with vinblastine-free flow medium. Nevertheless, the pronounced metabolic down regulation which had started already during the stimulation phase continued in wild-type and in transfected cells. Figure 5B shows the ECAR signals in *MDR1*-transfected cells as a function of time for different concentrations of vinblastine, and Figure 5C shows the evaluation of two different metabolic effects observed in *MDR1*-transfected cells. The upper solid line is the fit to the modified Michaelis−Menten equation (eq 1) and represents Pgp activation. The estimated concentration of half-maximum activation is somewhat higher than that for plasma membrane vesicles. The lower line is a fit to a Hill equation with an estimated half-

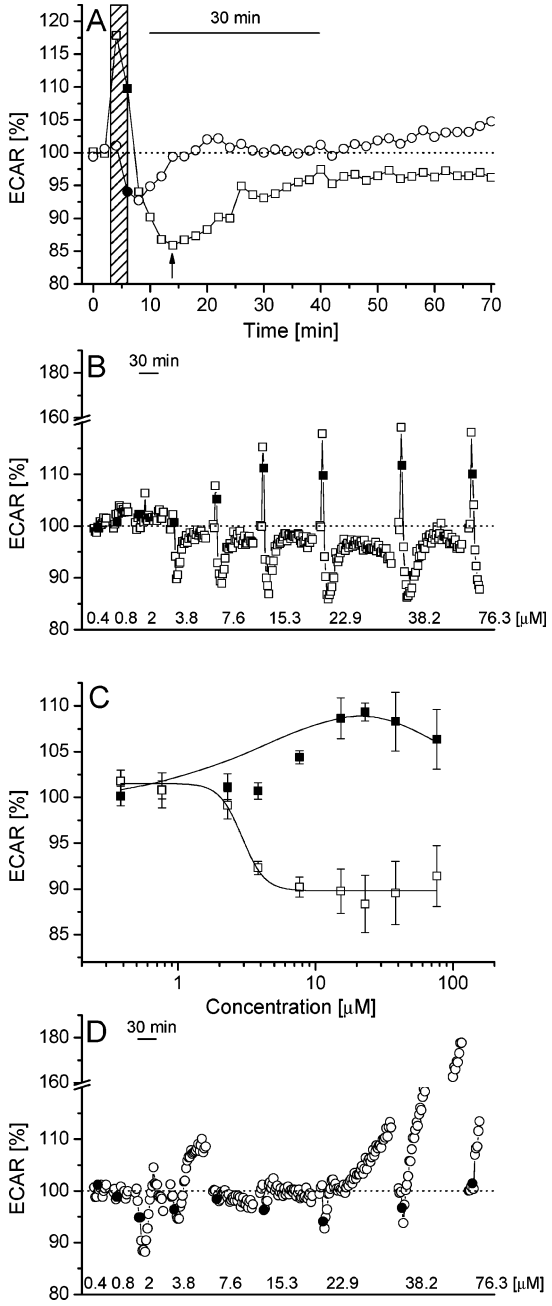

FIGURE 5: Time dependent ECAR of NIH-MDR1-G185 and NIH3T3 cells in response to increasing concentrations of vinblastine measured with a Cytosensor microphysiometer. A: ECAR of NIH-MDR1-G185 (squares) and NIH3T3 cells (circles) stimulated with 22.9 μM vinblastine as a function of time. The hatched box indicates the 3 min vinblastine stimulation period which comprises two measurement points, where the second measurement point is indicated as a filled symbol and is used for evaluation of Pgp activity if not otherwise stated. After the 3 min drug stimulation period cells were flushed again with drug-free flow medium. B: Time dependent ECAR of NIH-MDR1-G185 cells with increasing concentration of vinblastine (same type of measurement as in (A) but performed at different concentrations). C: ECAR of NIH-MDR1-G185 cells as function of vinblastine concentration. The second measurement point under vinblastine stimulation (■) most likely reflects Pgp activity and was fitted to a modified Michaelis−Menten equation (eq 1). The fit takes into account an estimated value for vinblastine adsorption to the Cytosensor tubing and debubbler membranes. Open squares (□) represent the fourth measurement point (indicated by arrow in (A)) and are fitted to a Hill equation. D: Time dependent ECAR of NIH3T3 cells with increasing concentration of vinblastine. The second measuring point is indicated as filled circles (●). Thirty minute time bars are included.

maximum inhibitory constant, $IC_{50} \approx 2.9$ μM, and may represent the inhibition of proton excretion by microtubules (*34*).

In wild-type cells (Figure 5D) low vinblastine concentrations caused a decrease in the ECAR which may again be attributed to the inhibition of proton excretion by microtubules starting, however, at even lower concentrations than in *MDR1*-transfected cells. Higher concentrations of vinblastine induced a strong continuous acidification which seems to be superimposed to the decrease in acidification at low concentrations. This strong continuous ECAR increase is typical for cell poisoning. Except daunorubicin, the other drugs measured so far showed no significant metabolic effects in wild-type cells (*24*).

DISCUSSION

We measured the activity of Pgp in inside-out vesicles formed from plasma membranes of mouse embryo fibroblasts (NIH-MDR1-G185) by monitoring the phosphate release rate for comparison with the Pgp activity measured previously in the corresponding living cells by monitoring the ECAR (*24*). For the present analysis Pgp was stimulated in a concentration-dependent manner with 19 different drugs, including cytotoxic compounds. Data were evaluated with a model proposed by Litman et al. (*19*) which assumes basal Pgp activity in the absence of drugs, activation of Pgp at low drug concentrations due to drug binding to a first binding region located in the cytosolic membrane leaflet, and inhibition at high drug concentrations due to drug binding to a second binding region (cf. eq 1). The large set of kinetic parameters is then used to get better insight into the relation between drug binding to the TMDs and ATP hydrolysis at the NBDs.

Comparison of the Kinetic Parameters from Plasma Membrane Vesicles and Living Cells. The comparison of Pgp activity in inside-out plasma membrane vesicles and living cells is shown in Figure 6A,B. The measurements in intact cells were performed at pH 7.4 (*24*), whereas the present phosphate release measurements were performed at pH 7.0. The slightly more acidic conditions were chosen to minimize drug association (cf. Materials and Methods) and vesicle aggregation (cf. Results). The basal activity of Pgp is practically not affected by the small pH difference as seen in Figure 4A which is in good agreement with previous investigations (*33*).

For the uncharged compounds or compounds with low ionization constants ($pK_a \leq 8.5$) (open symbols) the *concentrations of half-maximum activation*, K_1, are identical within error limits, with the exception of three outliers, daunorubicin (*5*), lidocaine (*9*), and progesterone (*10*), which showed higher K_1 values in the phosphate release assay than expected. Daunorubicin and progesterone self-associate at high concentrations. Self-association may also partially explain the large divergence of published concentrations of half-maximum activation for daunorubicin (*19*, *33*, *35*). Daunorubicin moreover induces metabolic effects in living NIH3T3 and NIH-MDR1-G185 cells above 10 μM (*24*) which coincide with the concentration range of Pgp activity in plasma membrane vesicles. The hydrophilic local anesthetic, lidocaine, had to be applied up to high concentration ($C_{sw} > 1$ mM), which exhausted the buffer capacity of the

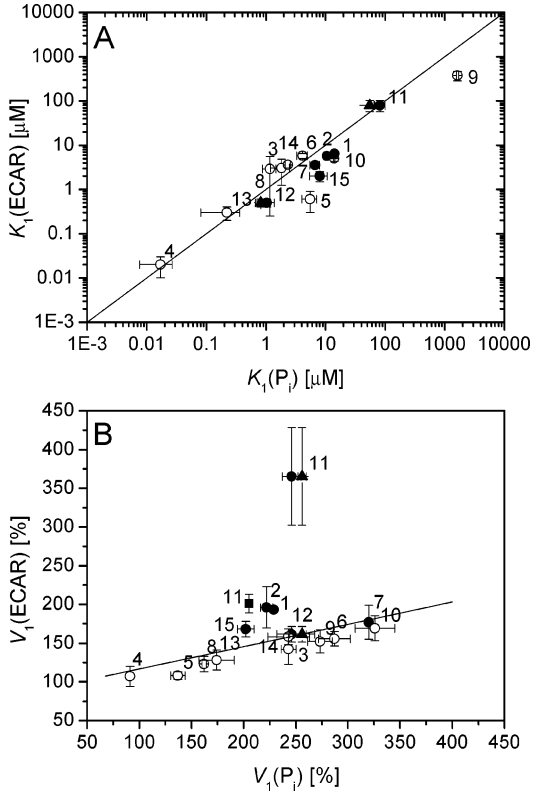

FIGURE 6: Comparison of kinetic data obtained with living cells (*24*) and inside-out membrane vesicles of NIH-MDR1-G185 cells. A: The concentration of half-maximum activation, K_1. B: Maximum Pgp activity, V_1. Phosphate release and ECAR assay, respectively, were performed at $T = 37$ °C, pH 7.0 and $T = 37$ °C, pH 7.4. Open circles (○) represent drugs with p$K_a \leq 8.5$, filled circles (●) drugs with p$K_a > 8.5$. Triangles (▲) represent values obtained with the phosphate release assay performed at pH 7.4. Data are expressed as the average of 2−15 measurements. The solid line in (A) is the diagonal to guide the eye, in (B) it is a linear fit without promazine (*11*). The Pgp activation profile for dibucaine (*6*) obtained from Cytosensor measurements was fitted to the simple Michaelis−Menten equation. In (B) the Pgp activation profiles for promazine (■) obtained from the Cytosensor and phosphate release assay, respectively, are also fitted to the simple Michaelis−Menten equation for comparison.

phosphate release buffer and led to an acidification of the solution (pH 6.83). As a result the lipid−water partition coefficient, K_{lw}, of the cationic compound decreased and the aqueous concentration required for half-maximum Pgp activation, K_1, increased concomitantly.

In the case of the highly charged compounds (p$K_a > 8.5$) (filled circles) the concentrations of half-maximum activation, K_1, were generally somewhat higher in the phosphate release assay (pH 7.0 at 37 °C) than in the ECAR assay (pH 7.4 at 37 °C), since the lipid−water partition coefficient, K_{lw}, was lower and the concentration for half-maximum Pgp activation, K_1, was higher. To illustrate the effect of the pH the K_1 values for verapamil and promazine obtained from phosphate release measurements performed at pH 7.4 (Figure 4B) were included in Figure 6A (filled triangles). As expected the K_1 values of the charged compounds moved to lower values and were in excellent agreement with those obtained by ECAR measurements (pH 7.4). In the pH range investigated the effect of pH on the activity of Pgp can therefore be attributed entirely to the pH dependence of the lipid−water partition coefficients, K_{lw}. Taking into account the possible artifacts and the pH difference, the concentrations of half-maximum activation obtained in plasma membrane vesicles and living cells are in good agreement over the broad range investigated ($K_1 \sim 10^{-8}$ M for cyclosporin A to $K_1 \sim 10^{-3}$ M for lidocaine) (Figure 6A). The fact that exogenous substrates (e.g., drugs) approach Pgp from the extracellular side in living cells and from the cytosolic side in inside-out cellular membrane vesicles does not play a role, as long as the molecules can deprotonate and cross the bilayer in their uncharged form (*2*). The membrane concentration of substrates (which is much higher than the aqueous concentration) can thus be assumed to be identical in the two different systems.

Figure 6B shows a comparison of the maximum activities, V_1, expressed as relative values ([%] of the basal value). A good linear correlation is observed, whereby promazine (*11*) is an outlier. In the phosphate release assay the V_1 value of promazine was too low due to vesicle aggregation (cf. Figure 3). In the ECAR assay the V_2 value was too low due to an acidification of the medium at high promazine concentrations which led in turn to a too high V_1 value. Data evaluation using simple Michaelis−Menten kinetics (neglecting the inhibitory part) yields comparable V_1 values (see filled square in Figure 6B). Overall, the relative rates of Pgp activity, V_1, are higher in plasma membrane vesicles than in living NIH-MDR1-G185 cells since the basal phosphate release rates are lower than the basal ECARs which include basal Pgp activity and all other metabolic processes of the cell.

Pgp activity expressed as phosphate released per total protein concentration and time was determined as $V_0 = (12.3 \pm 1.3)$ nmol·mg^{-1}·min^{-1} ($n \approx 126$). Taking into account an average number of $(1.9 \pm 0.3) \times 10^8$ cells/mL, a molecular weight of 170 kDa, and 1.95×10^6 molecules of Pgp per cell, the basal and maximum verapamil-stimulated turnover number was calculated as 3.4 s^{-1} and 5.2 s^{-1}, respectively. Ambudkar et al. (*27*) and Al-Shawi et al. (*1*) obtained slightly lower basal (2.9 s^{-1} and 2.75 s^{-1}, respectively) and higher verapamil-stimulated values (9.9 s^{-1} and 8.8 s^{-1},[2] respectively). The differences may be due to the different lipid composition and the different lateral packing density of the membranes.

In living cells the ECAR was measured in the presence of pyruvate which reduces the basal value by (50−60)%. The basal ECAR obtained with the Cytosensor was in the absence and presence of pyruvate $((3.0 \pm 0.6) \times 10^7)$ H$^+$·cell^{-1}·s^{-1} and $((1.4 \pm 0.6) \times 10^7)$ H$^+$·cell^{-1}·s^{-1}, respectively (*2*). The drug-stimulated ECAR was linearly related to the basal value at low acidification rates. However, it flattened out at high basal acidification rates (Figure 9[3] in ref *2*). Since the buffer capacity of the medium was low, the solution acidified, which led in turn to a decrease in the ECAR (*36*, *37*). This negative feedback was recently corroborated by ^{13}C NMR measurements using ^{13}C-labeled glucose (unpublished result, G. Kohler, P. Äänismaa, A. Seelig, and J. Seelig). The maximum verapamil-stimulated turnover number measured with the Cytosensor in the

[2] The turnover number corresponds to the measured maximum Pgp activity for verapamil taken from Figure 1 in ref *1*.

[3] Verapamil-induced and basal ECAR in buffer with glucose without pyruvate (g+) is an average of data obtained with cells of low and high passage numbers whereas the other data points were obtained with cells of high passage numbers. If only data from high passage numbers were used, the value was higher (*2*).

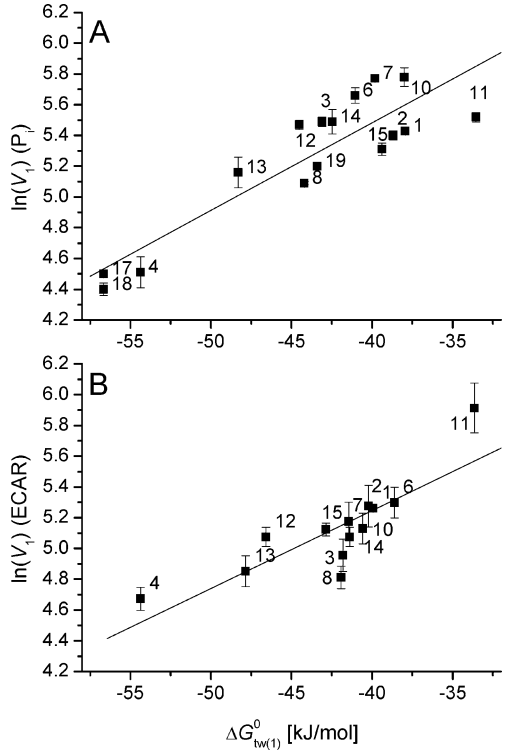

FIGURE 7: Correlation between the logarithm of the maximum Pgp activity, ln(V_1), obtained from phosphate release measurements at pH 7.0 (A) and from ECAR measurements at pH 7.4 (B) vs the free energy of drug binding from water to transporter, $\Delta G^0_{tw(1)}$. The maximum activity of Pgp, V_1, is expressed as a percentage of the basal rates taken as 100%. Data are presented as average of 2−15 measurements. Solid lines are linear regressions to the data with (A) a slope 0.06 ± 0.01 and an intercept 7.76 ± 0.34 (R = 0.89 ± 0.20) and (B) a slope 0.05 ± 0.01 and an intercept 7.27 ± 0.44 (R = 0.83 ± 0.18). Daunorubicin (*5*), lidocaine (*9*), and colchicine (*16*) are excluded from the fit in (A), and daunorubicin (*5*) and lidocaine (*9*) are excluded from the fit in (B) (cf. Results and Discussion).

presence of pyruvate (4.3 s^{-1}) was in close agreement with the number obtained with the phosphate release assay (5.2 s^{-1}). The effective value estimated from ECAR measurements in the absence of pyruvate must therefore be at least twice as large as supported by NMR measurements.

The Maximum Rate of ATP Hydrolysis by Pgp Depends on the Binding Affinity of the Drug from Water to the Transporter. To investigate the interplay between ATP hydrolysis at the NBDs and substrate binding and release at the TMDs, the maximum rate of Pgp activity, V_1 (Log scale), measured in inside-out membrane vesicles (at pH 7.0) and in living cells (at pH 7.4) was plotted as a function of the free energy of binding of the drug from the aqueous phase to the activating binding region of the transporter, $\Delta G^0_{tw(1)}$ (Figure 7A,B). The values of $\Delta G^0_{tw(1)}$ were derived from the concentration of half-maximum activation, K_1, as discussed previously (*24*). A linear correlation is observed which shows that the rate of phosphate release (Log scale) decreases with decreasing free energy of binding of the drug from water to the transporter, $\Delta G^0_{tw(1)}$ (or increasing binding affinity of the drug from water to the transporter).

A similar result was obtained previously by plotting the rate of Pgp activity either vs the free energy of binding from the lipid membrane to the transporter, $\Delta G^0_{tl(1)}$ (*17*), or vs the estimated free energy of hydrogen bond formation between substrate and transporter (*10*, *38*). Since the value of ΔG^0_{lw} is rather constant for the majority of compounds, the two free energies, $\Delta G^0_{tl(1)}$ and $\Delta G^0_{tw(1)}$, tend to be linearly correlated (*24*). Litman et al. (*19*) have shown that the rate of intrinsic drug transport decreases with increasing molecular weight, which often correlates with the number of hydrogen bond acceptor groups in Pgp substrates and thus with the free energy, $\Delta G^0_{tl(1)}$. Exceptions are the so-called third generation inhibitors such as OC144-093 (cf. ref *17*) which show a very high affinity to the lipid membrane (E. Gatlik and A. Seelig, unpublished results) but only a moderate affinity from the lipid membrane to the transporter ($\Delta G^0_{lw} < \Delta G^0_{tl(1)}$). The classical "inhibitor" cyclosporin A exhibits in contrast an intermediate affinity for the lipid membrane and a high affinity from the lipid membrane to the transporter ($\Delta G^0_{lw} > \Delta G^0_{tl(1)}$). Since the free energy of binding from water to the transporter, $\Delta G^0_{tw(1)}$, which is the sum of ΔG^0_{lw} and $\Delta G^0_{tl(1)}$, is large for both, they are both effective so-called inhibitors.

The linear decrease of the rate of ATP hydrolysis (Log scale) with increasing binding affinity of the drug from water to the transporter (Figure 7A,B) suggests that drug release in the extracellular leaflet is the rate-determining step. This is consistent with the fact that high drug concentrations, which impede drug release, reduce the rate of ATP hydrolysis. It is also consistent with the fact that compounds such as cyclosporin A and OC144-093 with a high affinity from water to the transporter and thus a slow release from the TMDs function as inhibitors or modulators of Pgp. ATP hydrolysis to reset Pgp for a new transport cycle thus seems to start only after drug unloading.

REFERENCES

1. Al-Shawi, M. K., Polar, M. K., Omote, H., and Figler, R. A. (2003) Transition state analysis of the coupling of drug transport to ATP hydrolysis by P-glycoprotein, *J. Biol. Chem. 278*, 52629−52640.
2. Gatlik-Landwojtowicz, E., Aanismaa, P., and Seelig, A. (2004) The rate of P-glycoprotein activation depends on the metabolic state of the cell, *Biochemistry 43*, 14840−14851.
3. Gottesman, M. M., and Ambudkar, S. V. (2001) Overview: ABC transporters and human disease, *J. Bioenerg. Biomembr. 33*, 453−458.
4. Litman, T., Druley, T. E., Stein, W. D., and Bates, S. E. (2001) From MDR to MXR: new understanding of multidrug resistance systems, their properties and clinical significance, *Cell. Mol. Life Sci. 58*, 931−959.
5. Seelig, A., and Gerebtzoff, G. (2006) Enhancement of drug absorption by noncharged detergents through membrane and P-glycoprotein binding, *Expert Opin. Drug Metab. Toxicol. 2*, 733−752.
6. Urbatsch, I. L., Sankaran, B., Bhagat, S., and Senior, A. E. (1995) Both P-glycoprotein nucleotide-binding sites are catalytically active, *J. Biol. Chem. 270*, 26956−26961.
7. Senior, A. E., al-Shawi, M. K., and Urbatsch, I. L. (1995) The catalytic cycle of P-glycoprotein, *FEBS Lett. 377*, 285−289.
8. Raviv, Y., Pollard, H. B., Bruggemann, E. P., Pastan, I., and Gottesman, M. M. (1990) Photosensitized labeling of a functional multidrug transporter in living drug-resistant tumor cells, *J. Biol. Chem. 265*, 3975−3980.
9. Rosenberg, M. F., Callaghan, R., Modok, S., Higgins, C. F., and Ford, R. C. (2005) Three-dimensional structure of P-glycoprotein: the transmembrane regions adopt an asymmetric configuration in the nucleotide-bound state, *J. Biol. Chem. 280*, 2857−2862.
10. Omote, H., and Al-Shawi, M. K. (2006) Interaction of Transported Drugs with the Lipid Bilayer and P-Glycoprotein through a Solvation Exchange Mechanism, *Biophys. J. 90*, 4046−4059.

11. Urbatsch, I. L., Tyndall, G. A., Tombline, G., and Senior, A. E. (2003) P-glycoprotein catalytic mechanism: studies of the ADP-vanadate inhibited state, *J. Biol. Chem. 278*, 23171−23179.
12. Higgins, C. F., and Linton, K. J. (2004) The ATP switch model for ABC transporters, *Nat. Struct. Mol. Biol. 11*, 918−926.
13. Sauna, Z. E., and Ambudkar, S. V. (2001) Characterization of the catalytic cycle of ATP hydrolysis by human P-glycoprotein. The two ATP hydrolysis events in a single catalytic cycle are kinetically similar but affect different functional outcomes, *J. Biol. Chem. 276*, 11653−11661.
14. Dey, S., Ramachandra, M., Pastan, I., Gottesman, M. M., and Ambudkar, S. V. (1997) Evidence for two nonidentical drug-interaction sites in the human P-glycoprotein, *Proc. Natl. Acad. Sci. U.S.A. 94*, 10594−10599.
15. Sharom, F. J., Lugo, M. R., and Eckford, P. D. (2005) New insights into the drug binding, transport and lipid flippase activities of the p-glycoprotein multidrug transporter, *J. Bioenerg. Biomembr. 37*, 481−487.
16. Seelig, A. (2006) Unraveling membrane-mediated substrate-transporter interactions, *Biophys. J. 90*, 3825−3826.
17. Seelig, A., and Gatlik-Landwojtowicz, E. (2005) Inhibitors of multidrug efflux transporters: their membrane and protein interactions, *Mini-Rev. Med. Chem. 5*, 135−151.
18. Omote, H., and Al-Shawi, M. K. (2002) A novel electron paramagnetic resonance approach to determine the mechanism of drug transport by P-glycoprotein, *J. Biol. Chem. 277*, 45688−45694.
19. Litman, T., Zeuthen, T., Skovsgaard, T., and Stein, W. D. (1997) Structure-activity relationships of P-glycoprotein interacting drugs: kinetic characterization of their effects on ATPase activity, *Biochim. Biophys. Acta 1361*, 159−168.
20. Kerr, K. M., Sauna, Z. E., and Ambudkar, S. V. (2001) Correlation between steady-state ATP hydrolysis and vanadate-induced ADP trapping in Human P-glycoprotein. Evidence for ADP release as the rate-limiting step in the catalytic cycle and its modulation by substrates, *J. Biol. Chem. 276*, 8657−8664.
21. Garrigues, A., Nugier, J., Orlowski, S., and Ezan, E. (2002) A high-throughput screening microplate test for the interaction of drugs with P-glycoprotein, *Anal. Biochem. 305*, 106−114.
22. Broxterman, H. J., and Pinedo, H. M. (1991) Energy metabolism in multidrug resistant tumor cells: a review, *J. Cell. Pharmacol. 2*, 239−247.
23. Landwojtowicz, E., Nervi, P., and Seelig, A. (2002) Real-time monitoring of P-glycoprotein activation in living cells, *Biochemistry 41*, 8050−8057.
24. Gatlik-Landwojtowicz, E., Aanismaa, P., and Seelig, A. (2006) Quantification and characterization of P-glycoprotein-substrate interactions, *Biochemistry 45*, 3020−3032.
25. McConnell, H. M., Owicki, J. C., Parce, J. W., Miller, D. L., Baxter, G. T., Wada, H. G., and Pitchford, S. (1992) The cytosensor microphysiometer: biological applications of silicon technology, *Science 257*, 1906−1912.
26. Ambudkar, S. V. (1998) Drug-stimulatable ATPase activity in crude membranes of human MDR1-transfected mammalian cells, *Methods Enzymol. 292*, 504−514.
27. Ambudkar, S. V., Cardarelli, C. O., Pashinsky, I., and Stein, W. D. (1997) Relation between the turnover number for vinblastine transport and for vinblastine-stimulated ATP hydrolysis by human P-glycoprotein, *J. Biol. Chem. 272*, 21160−21166.
28. Sharom, F. J., Yu, X., and Doige, C. A. (1993) Functional reconstitution of drug transport and ATPase activity in proteoliposomes containing partially purified P-glycoprotein, *J. Biol. Chem. 268*, 24197−24202.
29. Fischer, H., Gottschlich, R., and Seelig, A. (1998) Blood-brain barrier permeation: molecular parameters governing passive diffusion, *J. Membr. Biol. 165*, 201−211.
30. Gerebtzoff, G., Li-Blatter, X., Fischer, H., Frentzel, A., and Seelig, A. (2004) Halogenation of drugs enhances membrane binding and permeation, *ChemBioChem 5*, 676−684.
31. Yahya, A. M., McElnay, J. C., and D'Arcy, P. F. (1988) Drug sorption to glass and plastics, *Drug Metab. Drug Interact. 6*, 1−45.
32. Meier, M., Blatter, X. L., Seelig, A., and Seelig, J. (2006) Interaction of verapamil with lipid membranes and P-glycoprotein: connecting thermodynamics and membrane structure with functional activity, *Biophys. J. 91*, 2943−2955.
33. Al-Shawi, M. K., and Senior, A. E. (1993) Characterization of the adenosine triphosphatase activity of Chinese hamster P-glycoprotein, *J. Biol. Chem. 268*, 4197−4206.
34. Arruda, J. A., Sabatini, S., Mola, R., and Dytko, G. (1980) Inhibition of H+ secretion in the turtle bladder by colchicine and vinblastine, *J. Lab. Clin. Med. 96*, 450−459.
35. Romsicki, Y., and Sharom, F. J. (1999) The membrane lipid environment modulates drug interactions with the P- glycoprotein multidrug transporter, *Biochemistry 38*, 6887−6896.
36. Kaminskas, E. (1978) The pH-dependence of sugar-transport and glycolysis in cultured Ehrlich ascites-tumour cells, *Biochem. J. 174*, 453−459.
37. Wilhelm, G., Schulz, J., and Hofmann, E. (1971) pH-dependence of aerobic glycolysis in ehrlich ascites tumour cells, *FEBS Lett. 17*, 158−162.
38. Seelig, A., and Landwojtowicz, E. (2000) Structure-activity relationship of P-glycoprotein substrates and modifiers, *Eur. J. Pharm. Sci. 12*, 31−40.

BI0619526